NOVEL TECHNIQUES FOR SLURRY BUBBLE COLUMN HYDRODYNAMICS

First Annual Report for Grant DE-FG 22-95 PC 95212

July 1, 1996

SECTION IV: REPORRT FROM OHIO STATE UNIVERSITY (HEATT TRANSFER MEASUREMENTS)

L.S. Fan, S. Kuumar, D.J. Lee, P. Jiang, J. Reese
Department of CChemical Engineering
The Ohio State University
Columbus, Ohicio 43210

OBJECTIVE

A special heat transisfer probe is developed which is used to measure instantaneous local heat transfer coefficieients due to the passage of single gas bubbles injected in liquid and liquid-solid systems. AAlso the reliability and accuracy of the probe are validated.

INTRODUCTION

High heat transfer rarate is one of the most important characteristics in the operation of a slurry bubble column ı which results in effective reaction temperature control in such reactors. Fundamental hheat transfer studies have been concerned mainly with the measurement of time-averaaged heat transfer from the column wall to the bed and/or from the surface of immersed heeating object to the bed under steady state conditions. Due to inherent complexity of multiltiphase flow systems, however, little has been known in the past about the intrinsic mechaniism underlying the enhanced heat transfer in bubbling systems over non-bubbling systemsns. Therefore, a better understanding of the heat transfer behavior and the underlyingng mechanism is essential for the design, control, and optimum operation of such reactors.

The heat transfer pproperty in the bed is intimately associated with the bubble motion, bubble, size, and pphase holdups which are affected by fluid flow including wake flow. The wake flow behavvior, such as temporal variations in the shear flow at the bubble edge, chaotic primary wakeke, and vortex-vortex interaction, differs distinctively from the fluid flow behavior in the l bulk region (Fan and Tsuchiya, 1990). Thus, a fundamental understanding of bubble-ı-wake dynamics forms a necessary basis for a complete

description of various transnsport processes in these systems, and to predict fully the heat transfer performance of gaas-liquid and gas-liquid-solid systems, effects of bubble wake need to be considered. Thhe bubble wake effect on heat transfer can be quantified by the measurement of the instanintaneous local changes in the heat transfer coefficient, which depends strongly on the lococal hydrodynamics of the bed.

The complex behaavior of bubble columns is a direct result of the local flow structure which are time-vvariant due to the intrinsic dynamic behavior of the dispersed gas-phase motion and asssociated wake interaction. Therefore, to obtain a better understanding of the extreemely complex flow structure in bubble columns and its effects on the pertinent hydrodynaamic properties and heat transfer characteristics, it is necessary to understand a simplified l system involving a single bubble moving in liquid and liquid-solid systems.

To measure local iinstantaneous changes in heat transfer coefficients due to the passage of single gas bubbble, a special heat transfer probe is developed. This report highlights the design of the e novel heat transfer probe and its uniqueness and capability for accurately measuring the lolocal instantaneous heat transfer coefficients in multiphase flow systems. Moreover, discussssions of the mechanism of heat transfer enhancement due to the presence of bubble in simmplified systems involving single bubble injection in liquid and liquid-solid systems is presesented.

EXPERIMENTAL

A schematic diagram of the experimental apparatus is shown in Fig. 1. The experiments are performed in a three-dimensional Plexiglas column, 150 cm high and 1.62 cm ID. Liquid enters the column through a packed layer of 6 mm glass beads and a perforated-plate distributor ensuring uniform distribution of liquid in the column. The support for the fluidized particles is provided by a 200-mesh wire cloth. A steady liquid velocity is maintained by circulating water through a reservoir and a rotary pump. Tap water is used as the liquid phase in the experiments. Fluidized particles used are 163 μm (GB163) and 326 μm (GB326) glass beads. The physical properties of solid particles are given in Table 1.

Experiments involve single bubble injection in liquids and liquid-solid suspensions as shown in Figs. 2(a) and 2(b). A three-dimensional cup bubble injection system in Fig. 1 is designed in this study to introduce single bubbles without pressure perturbation or any satellites generation. A hemispherical cup of 2.5 cm diameter is inserted through the wall at 10 cm above the distributor. A known volume of air is injected into the cup through the stainless tube using a syringe. The trapped bubble is then released by turning the cup. The bubble volume varied from 3 cm^3 to 10 cm^3 with the corresponding bubble Reynolds number (based on equivalent bubble diameter) Re_b ranging from 5,300 to 9,000. Under these values of Re_b, the bubble is of spherical cap shape and the wake configuration is symmetric along the vertical axis of bubble. Furthermore, the bubbles rose almost rectilinearly. Miyahara *et al.* (1988) reported that for Re_b beyond 5,000 the bubble tends to discharge vorticity symmetrically and rises rectilinearly.

INSTANTANEOUS HEATT TRANSFER MEASUREMENT / PROBE DESIGN

The instantaneous loocal heat transfer rate is measured by a heat flow sensor/heater assembly (heat transfer probeie). Figure 3 shows the details of the probe design. The probe assembly consists of five commponents; microfoil heat flow sensor, copper plate, foil heater, thermosetting material (insulalator), and support. The foil heater is 2.54 cm high and 1.91 cm wide, and is heated by a cconstant voltage DC power source.

The local heat flux is s measured directly by a microfoil differential heat-flow sensor (RdF corporation, Model 204453-1; Table 2). The overall dimension of the sensor is 1.27 cm × 1.27 cm × 0.008 cm. ' This sensor utilizes thin foil type thermopile bonded to both sides of a known thermal b barrier (Fig. 4). The difference in temperature across the thermal barrier known, the seensor is factory-calibrated to provide the relation between the sensor output (voltage) and t the local heat flux (Fig. 5). The unique construction of the sensor provides it with low tl thermal capacitance (204.41 $J \cdot m^{-2}/K$), low thermal impedance (5.28×10^{-4} $m^2 \cdot K/W$), high seensitivity (8.56×10^{-3} $\mu V/W \cdot m^{-2}$), fast response time (0.02 s), and minimal thermal perturbaation to the heat flow. The microfoil heat flow sensor is flush mounted on the copper platete which is attached to the micro-foil heater and insulator as shown in Fig. 3.

The sensor can accurarately measure the heat flux and its surface temperature over a small surface area. The heateter/sensor probe assembly is usually positioned in the center of the column with the help of a a support as shown in Fig. 1. Due to the rectilinear motion of bubbles, there is a high probalability of bubbles striking the probe surface or at least passing very close to it. The probe i is located at about 50 cm from the point of bubble injection,

which allows sufficient distatance for the bubble to reach its terminal velocity (Miyahara *et al.*, 1988). Since the widtlth of the probe at a horizontal section of the column is small (0.32 cm), the disturbance to the flow in the vicinity of the probe is minimal and the fluidized state remains relatively undisturbed. A sheathed copper-constantan thermocouple located at tlthe column wall is used for the measurement of the bulk temperature. The average bibulk temperature is also monitored by a digital thermometer.

MEASUREMENT TECHNIQUE

Signals for the heat flux as well as the temperature difference between the probe surface and bulk are sampleed simultaneously at the rate of 186.2 Hz for 11 seconds. The signals from the sensor (typpically in microvolt range) are amplified to millivolts range by the amplifier/multiplexer sysystem (Metrabyte EXP-16) and interfaced with the high speed microcomputer data acquisitition system (Metrabyte DASH-16). Digital signals stored in the computer are convertedd to the corresponding heat transfer rate and the temperature difference using proper calibbration.

To reduce the higlgh frequency noise in the original signal, software signal processing is performed. Thhe signals are smoothed by employing a low-pass filter and the computations are performeded using Fast Fourier Transforms. A typical raw and filtered signal of the temperature difiifference ΔT_i (= T_{si} - T_∞) for a signal bubble injection in a liquid-solid fluidized bed containining GB163 is shown in Fig. 6. There is a significant change in temperature difference duee to the passage of bubble, but the change in q_i is not so significant compared to the temperature difference. Also, there is a large fluctuation in q_i

as compared to ΔT_i. Since the change in the instantaneous heat transfer rate depends on many factors including the thermal balance on both sides of the heater, the instantaneous heat transfer coefficient, h_i, is obtained from the instantaneous change in the temperature difference, ΔT_i, and the time averaged heat transfer rate, Q.

$$h_i = \frac{Q}{\Delta T_i} \tag{1}$$

Typical differential temperature ΔT_i in the stagnant liquid medium is 10°C, while that in the bubble column is 4°C. Due to the small dimension of the probe and minimal alteration in the hydrodynamic condition near the heat transfer surface, the measured instantaneous heat transfer coefficient in Eq. (1) is a direct measure of the local instantaneous heat transfer coefficients in the bed at that particular location. The local time-averaged heat transfer coefficient can be obtained by averaging the instantaneous heat transfer coefficient data over a number of sampling points (2048) as

$$h_{av} = \frac{1}{n}\sum_{i=1}^{n}\frac{Q}{\Delta T_i} \tag{2}$$

The small dimension of the probe (20 to 30 times smaller heat transfer area compared to conventional probes employed by Baker *et al.*, 1978 and Magliotou *et al.*, 1988), ease of installation, and high accuracy in measurements render its application limitless. For example, the probe could easily be positioned at any location in the bed to measure the instantaneous and time-averaged heat transfer coefficient. Also, since the heat transfer measurements are local in nature, the probe may be used for locating in-bed non homogeneity in a multiphase flow system. Thus, the probe is capable of instantaneous and local hydrodynamic characterization of a particulate multiphase reactor, thereby

providing significant informnation regarding the radial and axial variation of heat transfer in an industrial and pilot size r reactor which would be of enormous practical significance in better design and control of f such systems.

PROBE VALIDATION

The reliability and acccuracy of the probe are validated by performing heat transfer measurements in liquid (waater) systems and liquid-solid fluidized beds. Time-averaged local heat transfer coefficienmts in liquid-solid fluidized beds agree well with the immersed object-to-bed heat transfer r coefficients data and correlations reported in the literature (*e.g.*, Baker *et al.*, 1978 amnd Kato *et al.*, 1984). Also, a good agreement is obtained between the measured heat t transfer coefficient in stationary water with that predicted by the heat transfer correlationn for laminar free convection on a vertical plate immersed in stationary water reported in n the literature (*e.g.*, Incropera and De Witt, 1985).

INSTANTANEOUS HEAT TRANSFER COEFFICIENT

Figures 7, 8, and 9) show the instantaneous heat transfer coefficient due to the passage of a single gas bubbble in liquid, in liquid-solid systems containing GB163, and in liquid-solid systems containining GB326, respectively. The instantaneous heat transfer coefficient increased rapidly,y, attained a maximum value, and then gradually recovered to the initial value in liquid andd liquid-solid systems. It should also be noted from Figs. 7, 8, and 9 that due to the presence of secondary wake in liquid and liquid-solid systems, the heat transfer coefficient dooes not completely recover to the baseline value within the

sampling time of around 11 s. The effect of single bubble injection on heat transfer enhancement in the liquid system lasts much longer than in liquid-solid systems. Larger primary and secondary wakes and stronger vortex in such systems are primarily responsible for this phenommenon. All figures show that increased bubble volumn V_b causes increased enhancement due to larger bubble wake and stronger vortices.

Particle sizes in liquid-solid systems affect the bubble-wake induced heat transfer enhancement. In Figs. 8 and 9, heterogeneous effects caused by the larger particle size reduce the bubble-wake induced enhancement in heat transfer although the baseline value is increased. The baseline values (time-averaged heat transfer coefficient with no bubble injection) for liquid is 285 5 W/m^2·K, for GB163 system is 808 W/m^2·K, and for GB326 system is 815 W/m^2·K.

CONCLUDING REMARRKS

A novel heat tranansfer probe is developed which accurately measured the instantaneous changes in heteat transfer due to the passage of single gas bubble in liquid and liquid-solid systems. For a a bubble passing through the probe, the maximum heat transfer is observed in the wake regigion at a short distance behind the bubble in the upward flow of fluid rising along the wake central axis.

In both liquid and liquid-solid systems, the observed local maximum in the heat transfer coefficient behind a rising bubble is due to the effect of bubble wake. The local maximum in heat transfer, however, is more pronounced in liquid than in liquid-solid

systems. Also, the heat transfsfer enhancement due to the bubble passage increases with the bubble size due to larger bubblble wake and stronger vortices.

NOMENCLATURE

h_{av} time-averaged heat traiansfer coefficient over the sampling time, W/m^2·K

h_i instantaneous heat tranansfer coefficient, W/m^2·K

n number of sampling poioints, 2048

Q time-averaged heat fluxx, W/m^2

V_b bubble volume, cm^3

ΔT_i instantaneous temperaature difference between the probe surface (T_{si}) and bulk (T_∞), K

REFERENCES

C. G. J. Baker, E. R. Armstroong, and M. A. Bergougnou, "Heat Transfer in Three-Phase Fluidized Beds," *Powerer Technology*, **21**, 195 (1978).

L.-S. Fan and K. Tsuchiya,a, *Bubble Wake Dynamics in Liquids and Liquid-Solid Suspensions*, Butterwoorth-Heinemann, Stoneham, MA (1990).

F. P. Incropera and D. P. De VWitt, *Introduction to Heat Transfer*, 392, Wiley, NY (1985).

Y. Kato, Y. Taura, T. Kago,ɔ, and S. Morooka, "Heat Transfer Coefficient Between an Inserted Vertical Tubbe and a Three-Phase Fluidized Bed," *Kagaku Kogaku Ronbunshu*, **10**, 427 (1'1984).

M. Magiliotou, Y.-M. Chen, , and L.-S. Fna, "Bed-Immersed Object Heat Transfer in a Three-Phase Fluidized ɨ Bed," *AIChE J.*, **34**, 1043 (1988).

T. Miyahara, K. Tsuchiya, anɑd L.-S. Fan, "Wake Properties of a Single Gas Bubble in a Three-Dimensional Liqiquid-Solid Fluidized Bed," *Int. J. Multiphase Flow*, **14**, 749 (1988).

FIGURES AND TABLES S

Figure 1 A schematic c of experimental setup.

Figure 2 A schematic c of experimental conditions.

Figure 3 Heat-transferr probe design.

Figure 4 A schematic c of heat flow sensor.

Figure 5 Heat flow serensor calibration.

Figure 6 A typical raww and processed signal.

Figure 7 Effects of bulubble size on instantaneous heat-transfer coefficient due to the passage of buubble in liquid for probe located at the center of column.

Figure 8 Effects of bulubble size on instantaneous heat-transfer coefficient due to the passage of t bubble in liquid-solid fluidized bed with GB163 for probe located at thene center of column.

Figure 9 Effects of bulubble size on instantaneous heat-transfer coefficient due to the passage of t bubble in liquid-solid fluidized bed with GB326 for probe located at thene center of column.

Table 1 Physical propperties of spherical particles.

Table 2 Types of micicrofoil heat flow sensor.

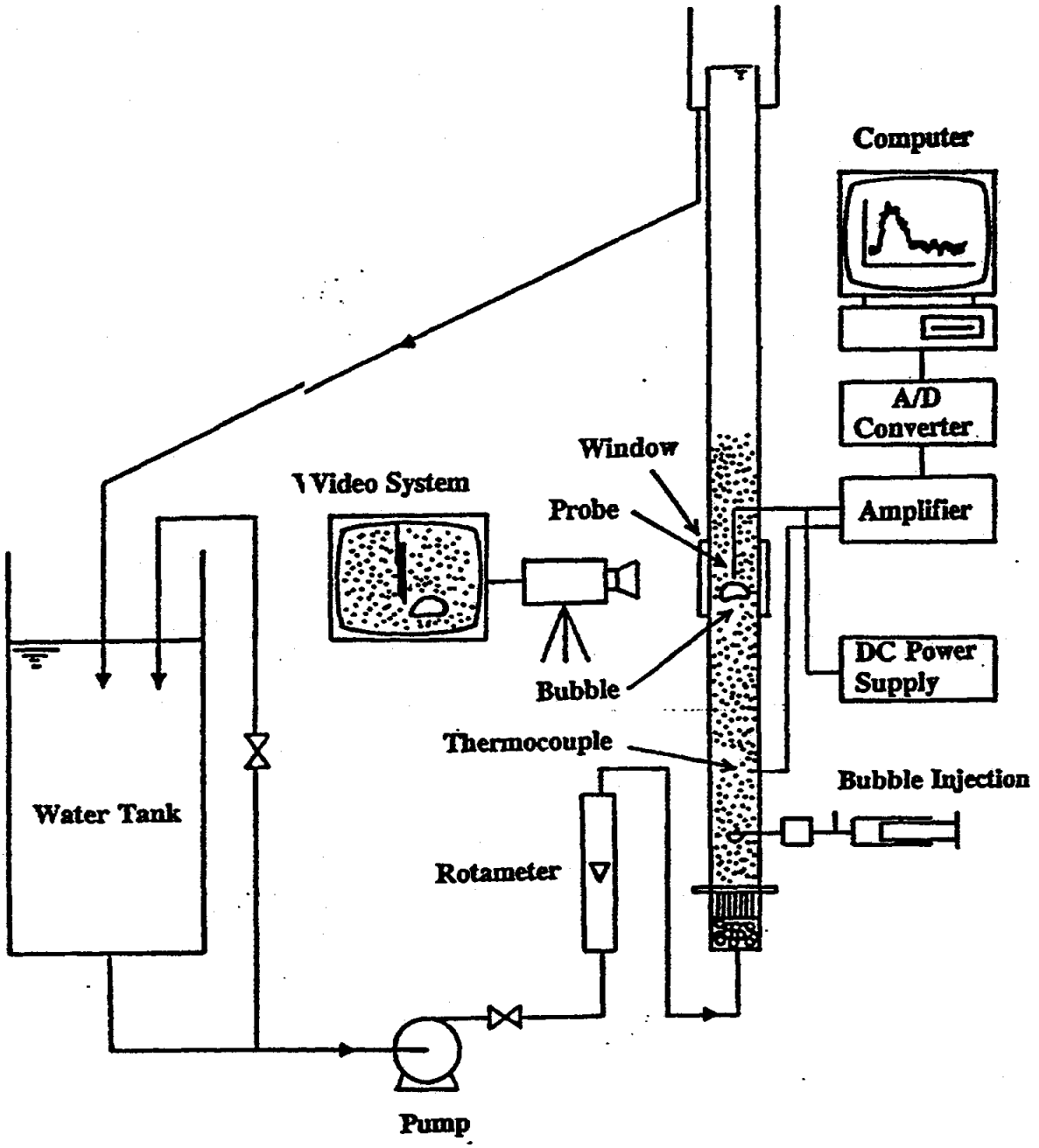

Figure 1 **A schematic of experimental setup.**

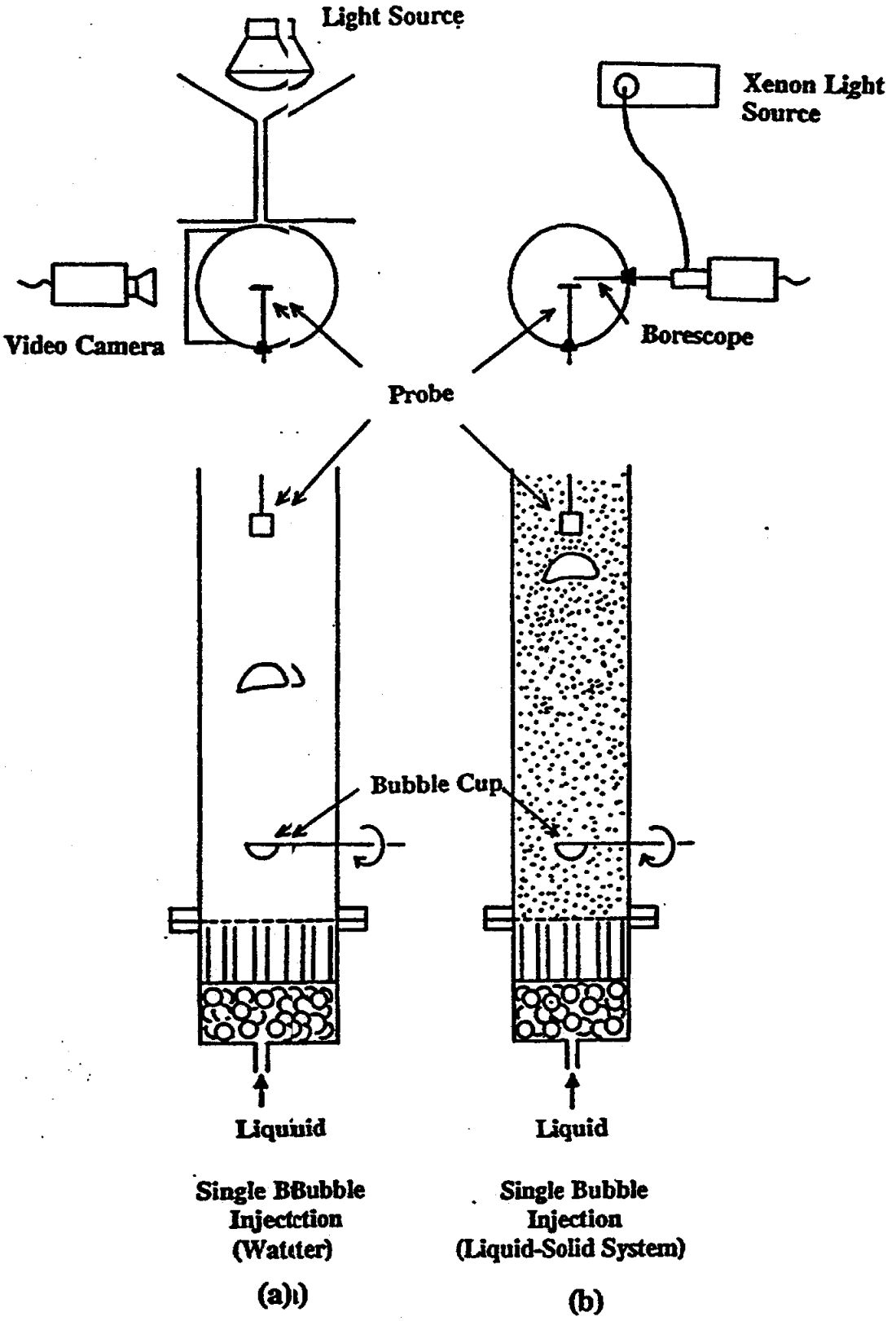

Figure 2 **A schematic of experimental conditions.**

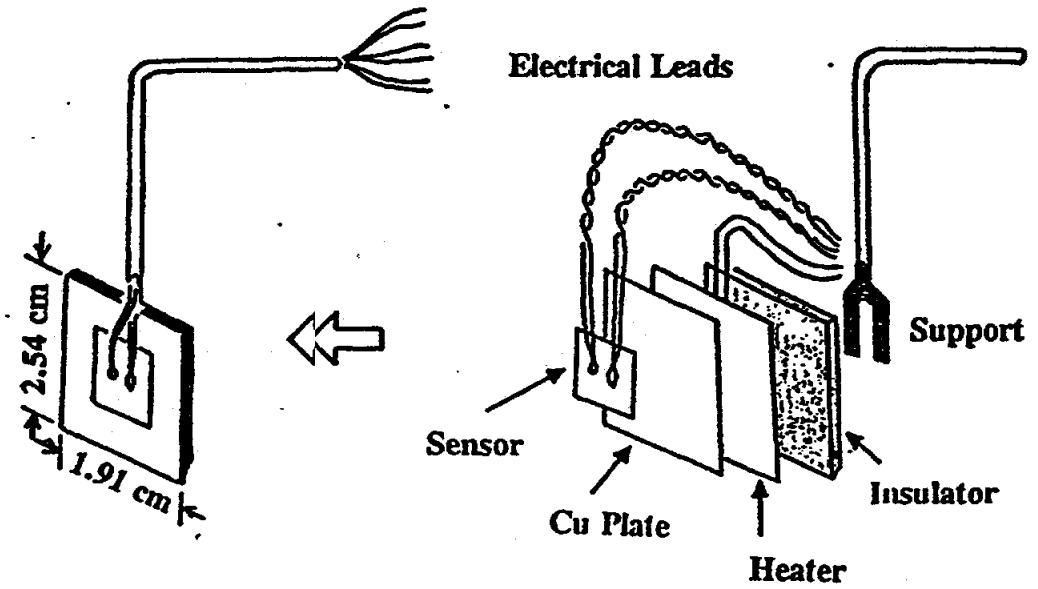

Figure 3 **Heat-transfer probe design.**

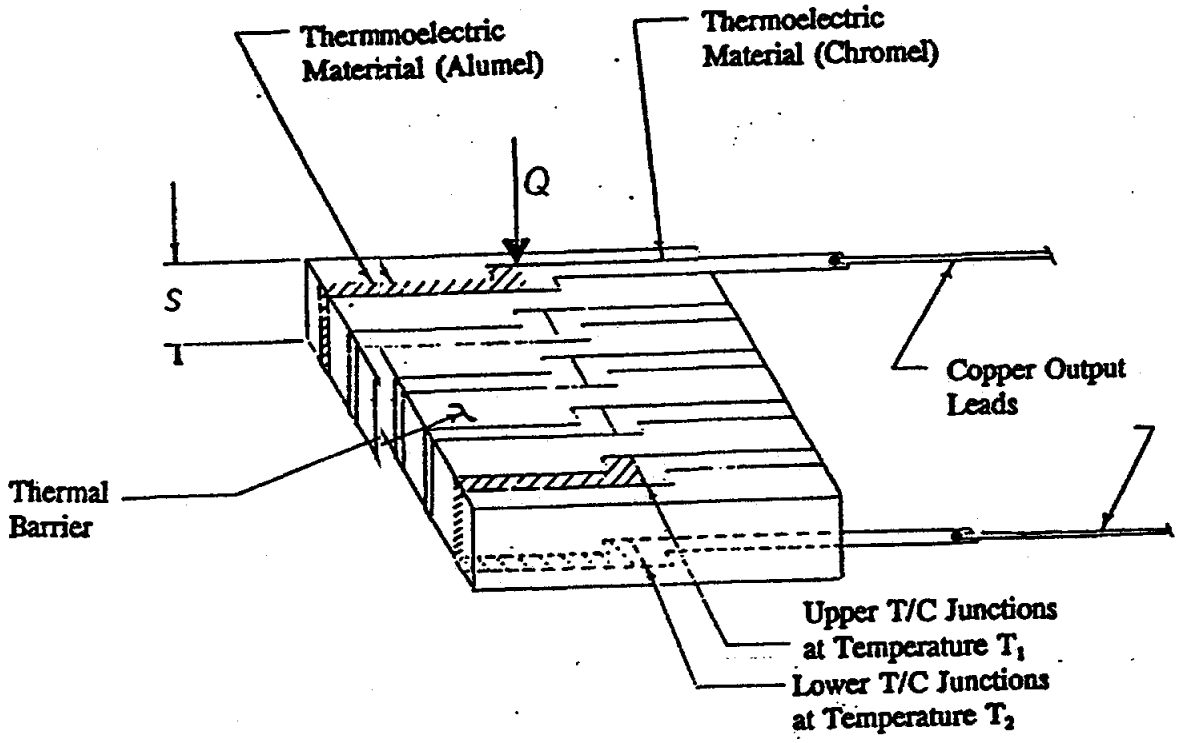

Figure 4 **A schematic of heat flow sensor.**

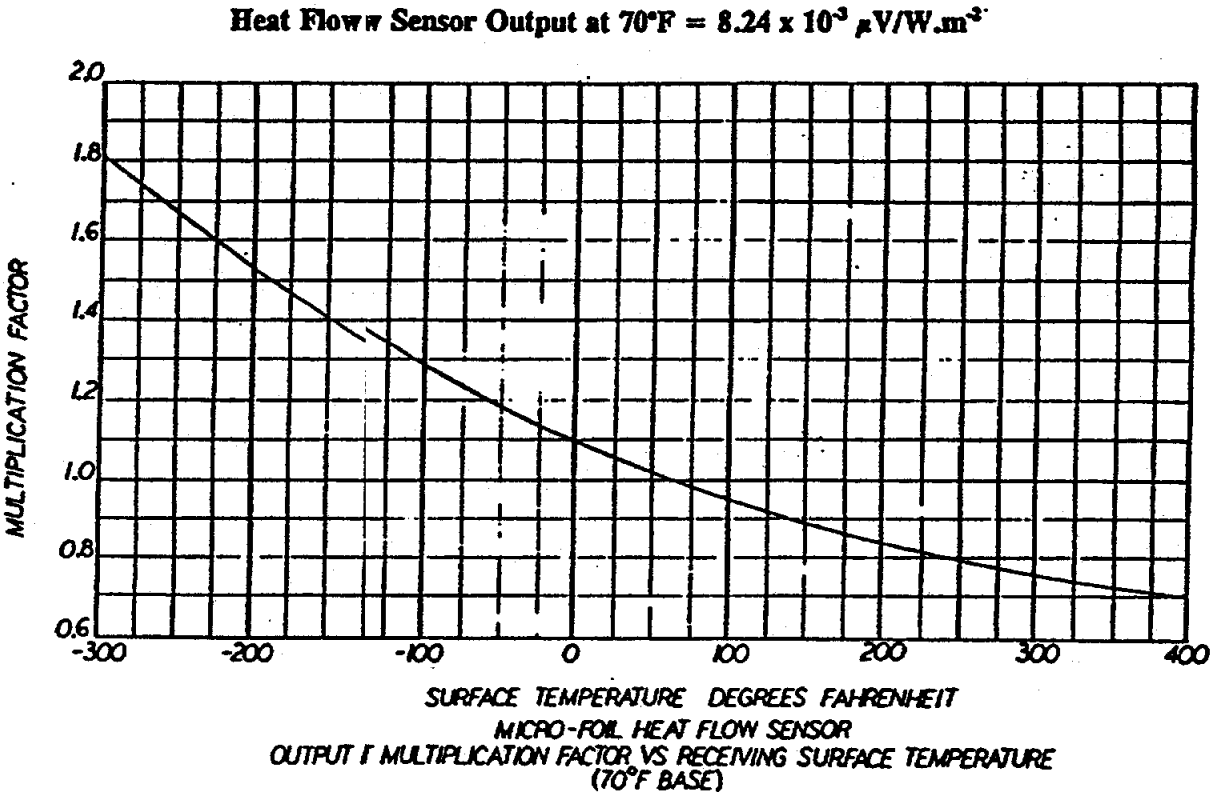

Figure 5 **Heat flow sensor calibration.**

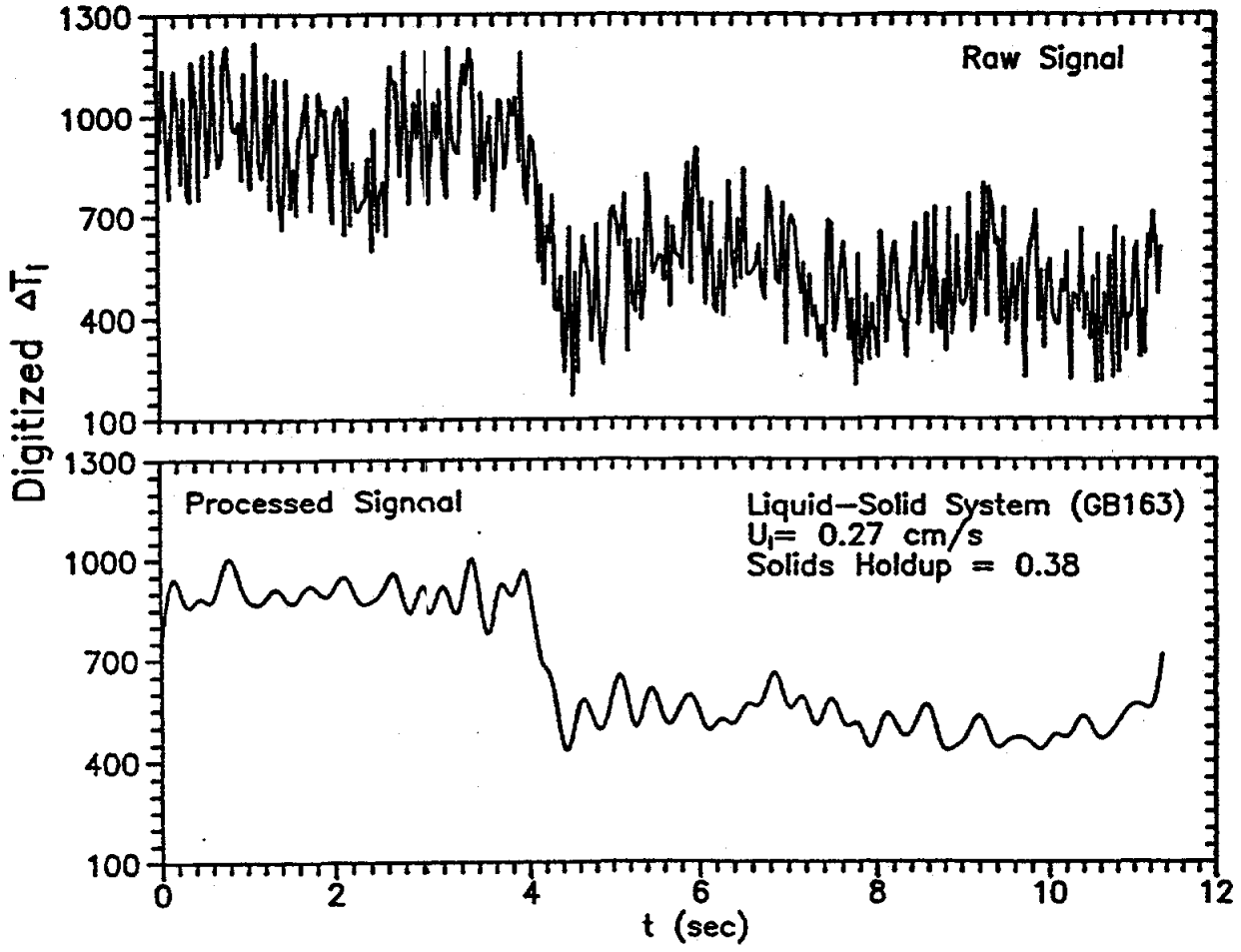

Figure 6 **A typical raw and processed signal.**

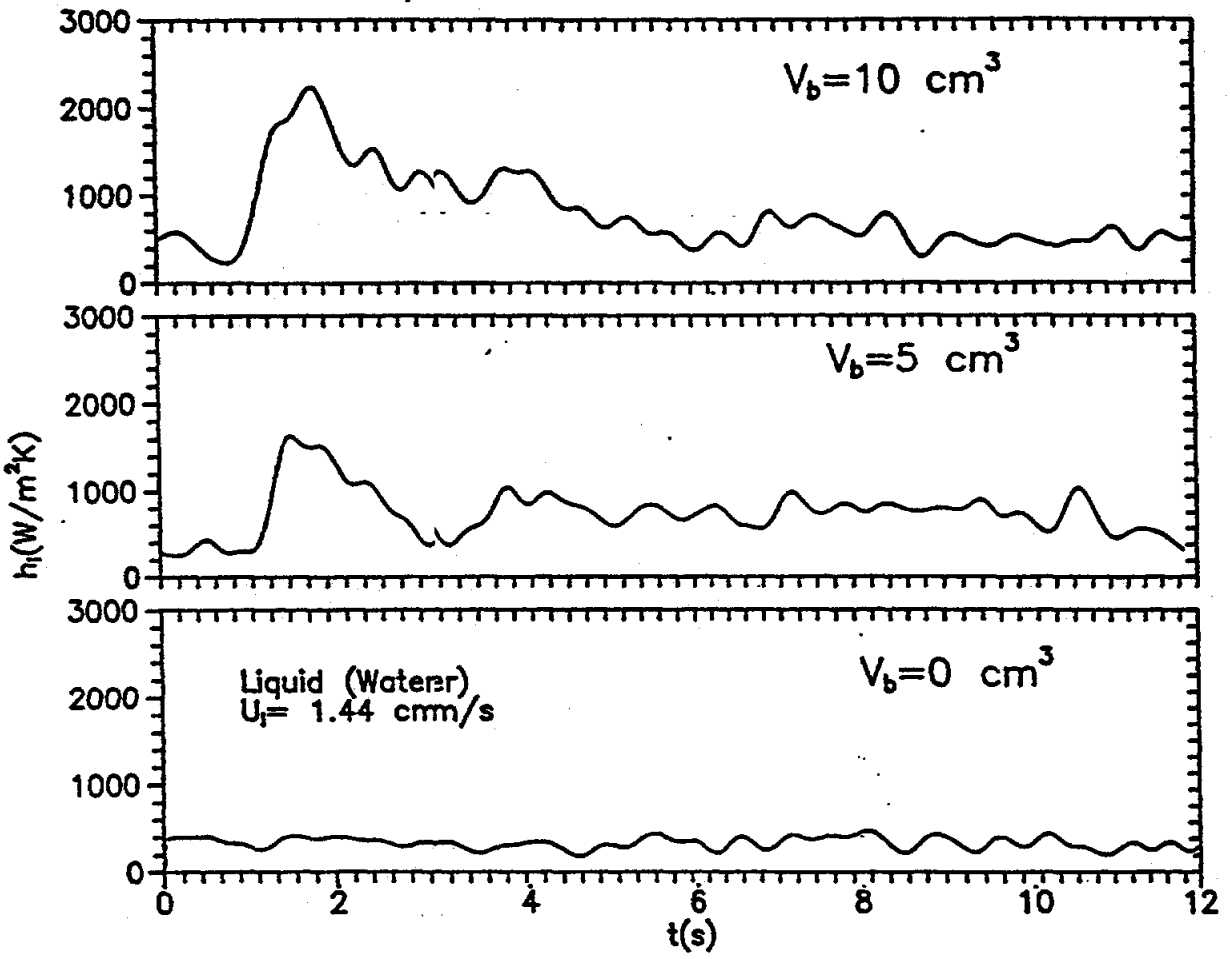

Figure 7 **Effects of bubbble size on instantaneous heat-transfer coefficient due to the passage of f bubble in liquid for probe located at the center of column.**

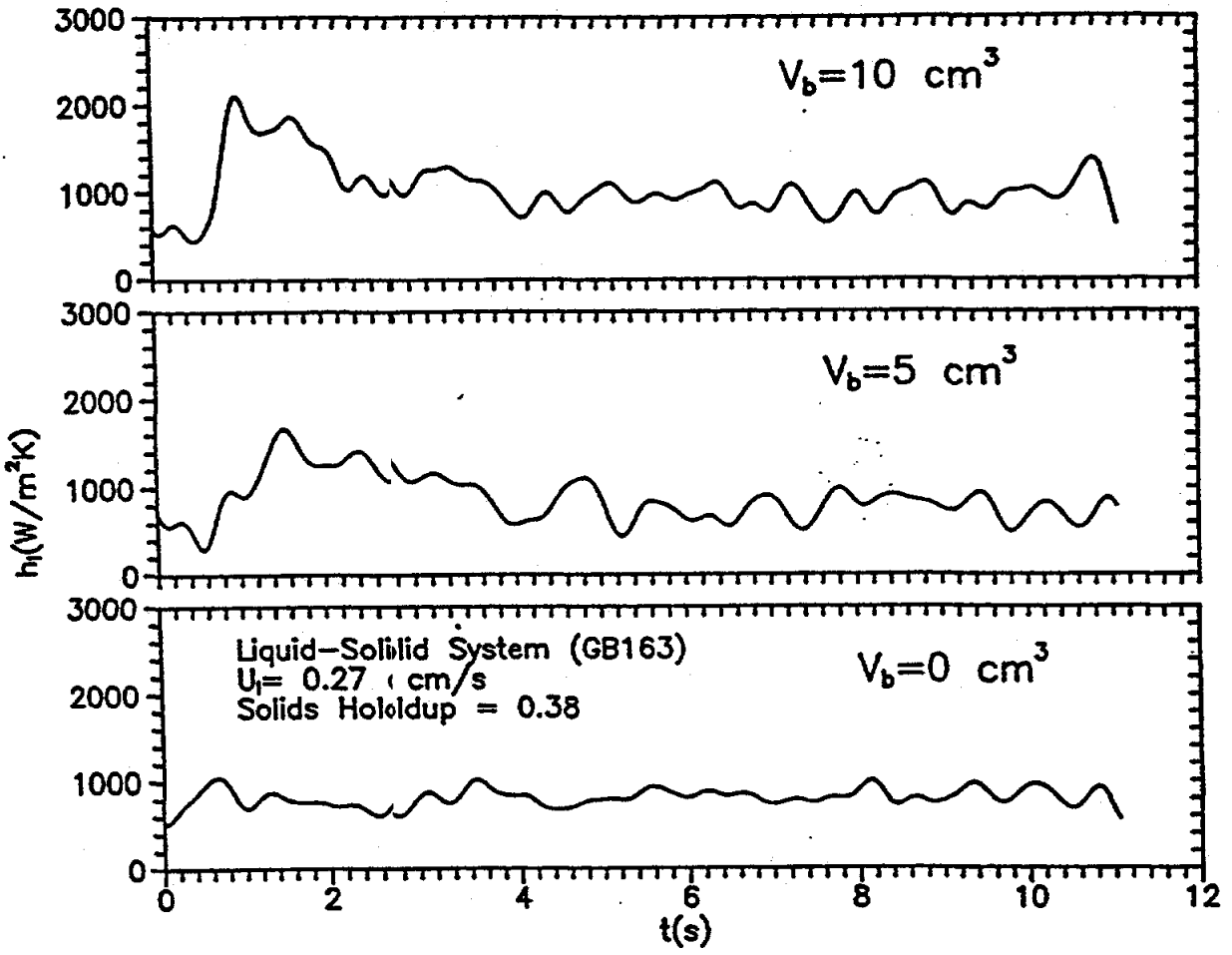

Figure 8 **Effects of bubble size on instantaneous heat-transfer coefficient due to the passage of bubble in liquid-solid fluidized bed with GB163 for probe located at the center of column.**

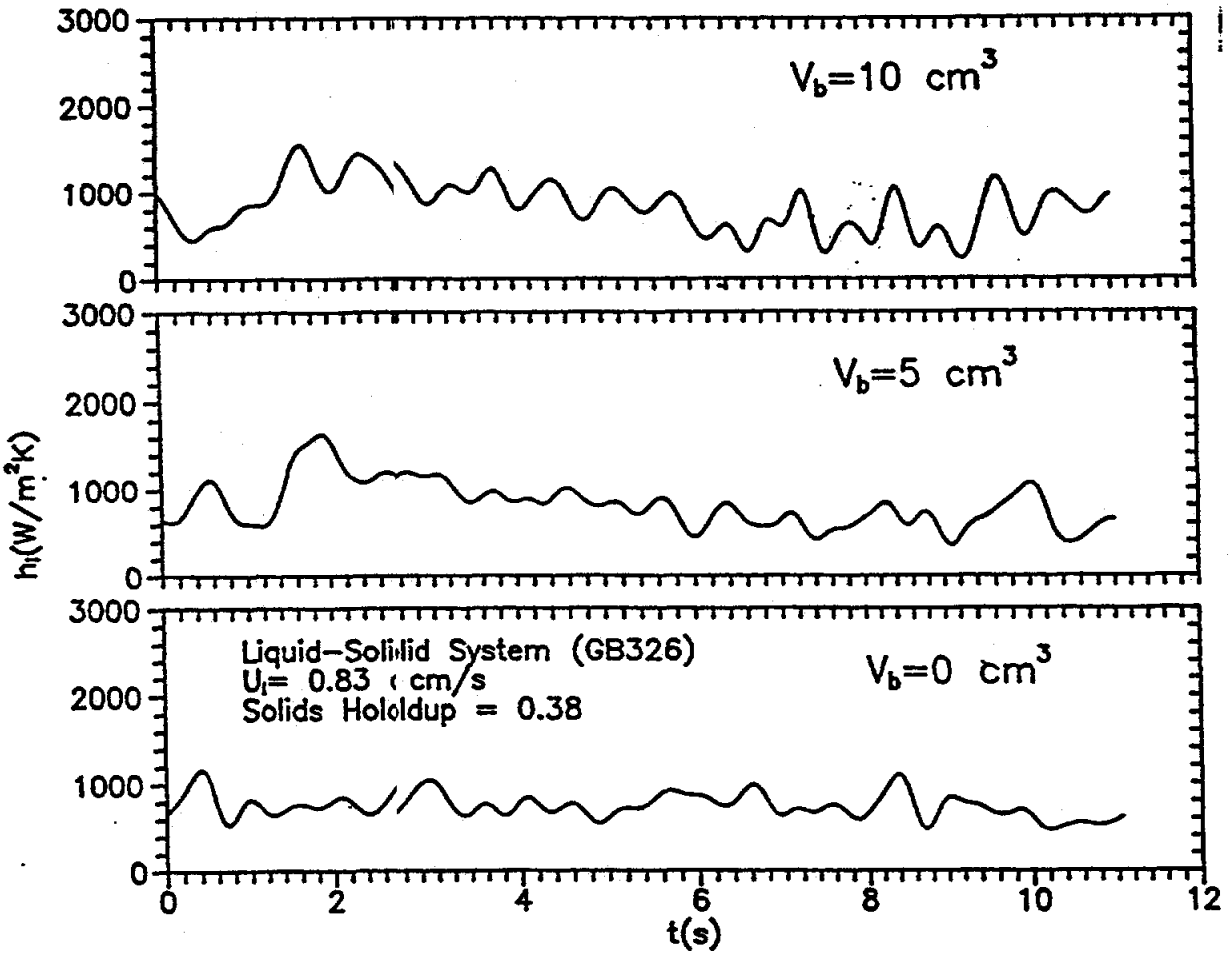

Figure 9 **Effects of buubble size on instantaneous heat-transfer coefficient due to the passage e of bubble in liquid-solid fluidized bed with GB326 for probe locateed at the center of column.**

Table 1 **Physicical properties of spherical particles.**

Particle	Notation	Average diameter (mm)	Density (g/cm^3)	ϵ_{s0}[a]	U_t[b] (m/s)
Glass bead	GB163	0.163	2.50	0.63	1.7×10^{-2}
Glass bead	GB326	0.326	2.50	0.62	4.4×10^{-2}

[a]Packed bed solids fraction
[b]Fan and Tsuchiya (1990)

Table 2 **Types off microfoil heat flow sensor.**

CONFIGURATION*	Part No/Number	Nominal Sensitivity (μv/Btu/ft²-hr.)	Maximum Recommended Heat Flux Btu/ft²-Sec.	Response Time (Seconds)	Sensor Resistance (Ω, Max.)	Maximum Operating Temp. (°F)	Nominal Thickness in (Inches)	Thermal Capacitance Btu / ft²-°F	Thermal Impedance Btu / °F per ft²-hr.
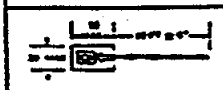	2040450-1	0.02	50	.020	5	500	.003	.01	.003
	2040450-2	0.06	25	.060	5	500	.005	.02	.005
	2040450-3	0.2	10	.400	5	500	.012	.05	.012
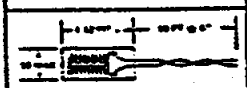	2040452-1	0.2	50	.020	20	500	.003	.01	.003
	2040452-2	0.6	25	.060	20	500	.005	.02	.005
	2040452-3	2.0	10	.400	20	500	.012	.05	.012
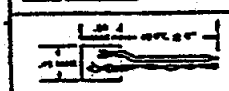	2040453-1	0.02	50	.020	5	500	.003	.01	.003
	2040453-2	0.06	25	.060	5	500	.005	.02	.005
	2040453-3	0.2	10	.400	5	500	.012	.05	.012
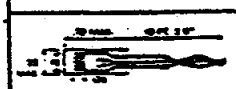	2707036-1	0.1	50	.020	10	500	.003	.01	.003
	2707036-2	0.3	25	.060	10	500	.005	.02	.005
	2707036-3	1.0	10	.400	10	500	.012	.05	.012
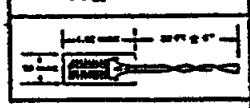	2040455-1	0.2	50	.020	20	500	.003	.01	.003
	2040455-2	0.6	25	.060	20	500	.005	.02	.005
	2040455-3	2.0	10	.400	20	500	.012	.05	.012
	2040456-1	1.1	50	.020	100	500	.004	.01	.003
	2040456-2	3.3	25	.060	100	500	.008	.02	.005
	2040456-3	11.0	10	.400	100	500	.013	.05	.012
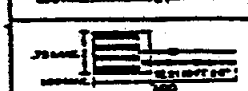	2040457-1	1.1	50	.020	100	500	.004	.01	.003
	2040457-2	3.3	25	.060	100	500	.008	.02	.005
	2040457-3	11.0	10	.400	100	500	.013	.05	.012
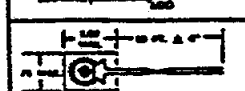	2040466-1	0.2	50	.020	15	500	.003	.01	.003
	2040466-2	0.6	25	.060	15	500	.005	.02	.005
	2040466-3	2.2	10	.400	15	500	.012	.05	.012
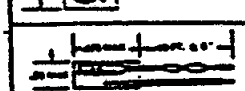	2040472-1	0.2	50	.020	90	500	.003	.01	.003
	2040472-2	0.6	25	.060	90	500	.005	.02	.005
	2040472-3	2.0	10	.400	90	500	.012	.05	.012
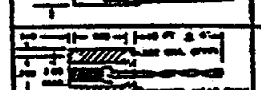	2040480-1	0.2	50	.020	20	500	.195	.01	.003
	2040480-2	0.6	25	.060	20	500	.195	.02	.005
	2040480-3	2.0	10	.400	20	500	.195	.05	.012